pp 785–797. © Royal Aeronautical Society 2018
doi: 10.1017/aer.2018.10

Application of optimal control law to laser guided bomb

Takieddine Mouada
mouadatakieddine@gmail.com
Military Academy, University of Defence
Belgrade
Serbia

Milos V. Pavic, Bojan M. Pavkovic, Sasa Z. Zivkovic and Mirko S. Misljen
Military Technical Institute
Belgrade
Serbia

ABSTRACT

The paper presents a laser guided bomb guidance law based on the linear quadratic differential game theory, where a case of two perpendicular planes with two state variables in each plane has been considered. The Kalman filtering method has been used for noise removal from the measured signals and for estimation of the missing state variable values needed for the optimal guidance law. Optimisation has been conducted with respect to minimisation of the performance index. Comparative analysis of different guidance laws is done. A statistical analysis is performed to obtain the terminal miss distance in dependence on total flight time.

Keywords: Proportional navigation; optimal guidance; missile control; line-of-sight rate estimation; laser guided bomb; Kalman filter; strap-down seeker

Received 24 April 2017; revised 31 January 2018; accepted 6 February 2018; first published online 13 March 2018.

https://doi.org/10.1017/aer.2018.10 Published online by Cambridge University Press

NOMENCLATURE

HE	Heading Error
PN	Proportional Navigation
LOS	Line of Sight
FOV	Field of View
SINS	Strap-down Inertial Navigation System
$\mathbf{A}$, $\mathbf{B}$, $\mathbf{D}$	state (system) matrix, control (input) matrix, and disturbance matrix
b, c	penalties imposed by the miss distance and the terminal normal velocity
$\mathbf{B}_k$	discrete control (input) matrix
g	gravitational acceleration, ms^{-2}
g_1, g_2, g_3	optimal guidance law gains
$\mathbf{H}$	measurement matrix
J	optimal control performance index
K_1, K_2, K_k	Kalman gains
$\mathbf{M}_k$	covariance matrix
N	navigation constant
n_k	achieved missile lateral acceleration
$\mathbf{P}_k$	covariance matrix
$\mathbf{P}_0$	initial covariance matrix
$\mathbf{Q}_k$	process noise matrix
r	range, m
$\mathbf{R}$	measurement noise matrix
$\mathbf{R}_k$	covariance matrix
u_k	guidance law
t	time, s
t_f	time final, s
T_s	simple time, s
t_{go}	time to go, s
u, w	lateral accelerations, ms^{-2}
V_c	closing velocity, ms^{-1}
$\mathbf{v}_k$	noise measurement vector
w_0	target manoeuvre, ms^{-2}
$\mathbf{x}$	state-space vector
x_0	initial distance, m
x_1, x_2	lateral relative displacement and relative velocity, m, ms^{-2}
x^*_{1k}	pseudo-measurement of relative position
$\hat{x}_{1k}$, $\hat{x}_{2k}$	estimated values of the state vector elements.
z_0	initial height, m
$\mathbf{Z}_k$	measurement vector
$\mathbf{\Phi}$	continuous transition matrix
$\mathbf{\Phi}_k$	discrete transition matrix
$\mathbf{\Phi}_s$	spectral density
λ	angle of line of sight rad
$\dot{\lambda}$,λ_1,λ_2	lOS rate
λ^*_k	measured LOS
η	demand fin deflection

https://doi.org/10.1017/aer.2018.10 Published online by Cambridge University Press

η_M	achieved lateral acceleration
η_c	achieved fin deflection
σ_n	variance of the measurement noise
σ_λ	Gaussian noise, mrad

1.0 INTRODUCTION

The precision guided expensive weapon plays a more and more important role in the modern war, so the development of missile guidance has become the focus of world militaries (see Ref. 1). Accuracy and precision of simple aerial bombs can be significantly improved by using the simple target tracking device and actuators for aerodynamic control surfaces. The Proportional Navigation (PN) is one of the commonly used guidance laws in practice. This law was used extensively in short and medium range homing missile guidance and control systems (see Refs 2 and 3). Trajectory tracking guidance laws presented in Ref. 4 were not suitable for homing, and only the pulse frequency modulation could be adopted. In the case of slowly manoeuvring ground targets, in Ref. 5, the pursuit guidance law was used as a guidance approach where the velocity vector always points to a target. The use of the pursuit guidance law implies attaching a statically stable aerodynamic sensor platform on the top of the aerial bomb, which always positions itself in the direction of the velocity vector. Laser seeker on this platform detects the angular deviation of the Line of Sight (LOS) from the velocity direction, and this information is used to calculate steering commands for trajectory correction. If the applied seeker has a large enough Field of View (FOV), it can be directly mounted on the top of the bomb, as shown in Fig. 1.

In this way, this bomb does not require any gimballed tracking system part, but only a strap-down seeker system which is defined in Ref. 6. Besides the seeker, the system must include a Strap-down Inertial Navigation System (SINS), see Ref. 7, with solid-state components and three rate gyroscopes. This system is mechanically less complex and more reliable. Such a system allows us to detect an angular deviation of LOS relative to the body-fixed coordinate frame and it cannot measure LOS rate ($\dot{\lambda}$). However, it gives information on the angle between the LOS and the centreline of the missile (ε). This information is used as the error input in the guidance loop. In Refs 8 and 9, a Kalman filter is used to eliminate noise from the measured LOS rate. In this paper, we used the Kalman filter to estimate the LOS rate, based only on the measurement of the angular error (corrupted with noise), because the major problem is lack of information on the LOS rate as guidance laws based on PN or optimal guidance require this rate as the input value.

The objective of this work is to obtain a low cost and efficient guidance system that would be used on short-range guided bomb. In this paper, an optimal guidance method is proposed, based on a strap down seeker system. This system allows the detection of the angle between the LOS and the centreline of the missile, while in the pursuit guidance system it is relative to the velocity vector. This angle (ε) was used as an input to the Kalman filter for noise removal from the measured signals and for estimating the LOS rate (Ref. 8). This value is required for optimal guidance. Finally, after signal filtration, estimation and guidance control calculation, the coordinate transformation is used in the opposite direction, from guidance to body reference system, where commands are executed.

This paper is organised as follows. Section 2 presents the general theoretical basics of linear quadratic differential games (LQDG) and their application in the algorithm of optimal

https://doi.org/10.1017/aer.2018.10 Published online by Cambridge University Press

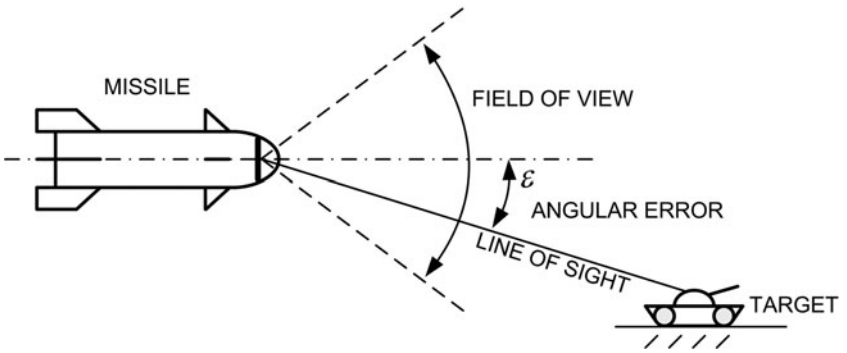


Figure 1. Strap-down (non-gimballed) homing head.

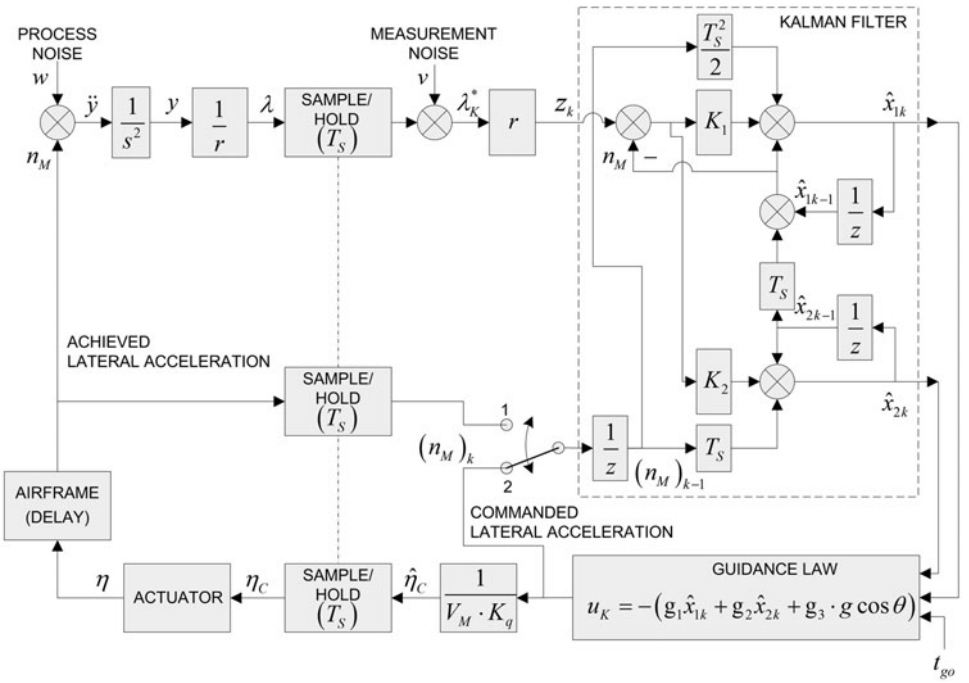


Figure 2. Second-order Kalman filter with position measurement only.

guidance law. In Section 3, the model of Kalman filter is used to eliminate noise from the measured signals and to estimate the LOS rate. The estimation of LOS rate, which is affected by the angle error, is needed for the optimal guidance law, which is shown in Fig. 2. In Section 4, the simulation results (lateral displacement, lateral velocity, trajectories, commanded lateral acceleration, terminal miss distance and deviation with different heading error) and the comparison with the different guidance methods are shown. Finally, Section 5 is devoted to the conclusions.

https://doi.org/10.1017/aer.2018.10 Published online by Cambridge University Press

2.0 OPTIMAL GUIDANCE

The motion of the missile-target system in one plane is described by the following differential equation in state space (Ref. 10):

$$\begin{gathered}\dot{\mathbf{x}} = \mathbf{A}\mathbf{x} + \mathbf{B}u + \mathbf{D}w \\ \mathbf{x}(t_0) = \left[\, x_1(t_0)\ x_2(t_0) \,\right]^{\mathrm{T}} \\ \mathbf{A} = \begin{bmatrix} 0 & 1 \\ 0 & 0 \end{bmatrix}, \quad \mathbf{B} = \begin{bmatrix} 0 \\ 1 \end{bmatrix}, \quad \mathbf{D} = \begin{bmatrix} 0 \\ 1 \end{bmatrix}\end{gathered} \qquad \ldots (1)$$

Scalar variables *x1* and *x2* are the components of the state vector **x**, which also represent the relative lateral displacement and the velocity, respectively, while *u* and *w* are the corresponding lateral accelerations of the bomb and the target.

As shown in Ref. 10, the optimal guidance problem is to minimise the following performance index:

$$J = \frac{b}{2}x_1^2(t_\mathrm{f}) + \frac{c}{2}x_2^2(t_\mathrm{f}) + \frac{1}{2}\int_{t_0}^{t_\mathrm{f}} u^2(t)\mathrm{d}t \qquad \ldots (2)$$

In the previous equation, $b > 0$ is a penalty imposed by the miss distance (i.e. the relative separation at the final time t_f); the coefficient $c > 0$ is introduced to minimise the terminal lateral velocity. In the case when $c < 0$, the bomb's objective is to maximise the velocity. The last component represents command during the flight, and minimises it.

For the perfect interception, $x_1(t_\mathrm{f}) = 0$, it is required that $b \to \infty$, and for the perfect rendezvous, besides the previous condition, there is also $x_2(t_\mathrm{f}) = 0$, and it is required that both penalty coefficients tend to infinity, i.e. $b \to \infty$, $c \to \infty$.

Assuming the target is manoeuvring with a constant lateral acceleration ($w = \mathrm{const} = w_0$) starting at $t = t_0$, the expression of guidance control value was obtained in Ref. 10, as the solution of a two-point boundary value, applying the given boundary conditions. These values are obtained by the following steps.

In the case of Performance index (2) minimising, the adjoin equations are:

$$\dot{\lambda}_1 = 0, \quad \dot{\lambda}_2 = -\lambda_1, \quad u = -\lambda_2 \qquad \ldots (3)$$

With the boundary conditions:

$$\lambda_1(t_\mathrm{f}) = bx_1(t_\mathrm{f}), \quad \lambda_2(t_\mathrm{f}) = cx_2(t_\mathrm{f}) \qquad \ldots (4)$$

Solving these two equations gives:

$$\begin{aligned}\lambda_1 &= bx_1(t_\mathrm{f}), \\ \lambda_2 &= bx_1(t_\mathrm{f})(t_\mathrm{f} - t) + cx_2(t_\mathrm{f})\end{aligned} \qquad \ldots (5)$$

And the control is:

$$u(t) = -\left[bx_1(t_\mathrm{f})(t_\mathrm{f} - t) + cx_2(t_\mathrm{f})\right] \qquad \ldots (6)$$

https://doi.org/10.1017/aer.2018.10 Published online by Cambridge University Press

Now, combining Equations (6) and (1), the expressions for $x_1(t)$ and $x_2(t)$ are obtained after integration from t_0 to t. After introducing the shift $t = t_f$, the unknown final values $x_1(t_f)$ and $x_2(t_f)$ are solved, and finally the control law in closed form was determined as:

$$\begin{aligned} u(t) &= -\left[g_1 x_1(t) + g_2 x_2(t) + g_3 w_0\right] \\ g_1 &= \frac{t_{go} b \left(\frac{1}{2} t_{go} c + 1\right)}{t_{go}^4 \frac{cb}{12} + t_{go}^3 \frac{b}{3} + t_{go} c + 1} \\ g_2 &= \frac{t_{go}^3 \frac{cb}{3} + t_{go}^2 b + c}{t_{go}^4 \frac{cb}{12} + t_{go}^3 \frac{b}{3} + t_{go} c + 1} \\ g_3 &= \frac{t_{go}^4 \frac{cb}{12} + t_{go}^3 \frac{b}{2} + t_{go} c}{t_{go}^4 \frac{cb}{12} + t_{go}^3 \frac{b}{3} + t_{go} c + 1} \end{aligned} \quad \ldots (7)$$

In the previous equations, $t_{go} = t_f - t$ is the time-to-go (remaining time until impact).

Now, it is considered the so-called "perfect rendezvous," where both the miss distance and the terminal velocity are minimised. In this case, from Equation (7) taking $b \to \infty$ and $c \to \infty$, feedback gains are obtained as:

$$g_1 = \frac{6}{t_{go}^2}, \quad g_2 = \frac{4}{t_{go}}, \quad g_3 = 1 \quad \ldots (8)$$

The control signal can be expressed as:

$$u = -V_c \left(4\dot{\lambda} + \frac{2}{t_{go}}\lambda\right) - w_0, \quad \ldots (9)$$

where V_c is the closing velocity. The previous equation represents optimal guidance with navigation constant $N = 4$ and an additional feedback from the LOS angle, also with compensation factor $1 \times w_0$ to cancel out the target acceleration effect by performing exactly the opposite manoeuvre. For slowly moving objects on the ground, gravity is modelled as effective target acceleration and, thus, known in advance. In this way, the gravity influence in the vertical plane is compensated.

3.0 EXTENDED KALMAN FILTER

The continuous fundamental matrix (continuous transition matrix) is obtained from the system matrix (Refs 11 and 12):

$$F(t) = \mathcal{L}^{-1}\{(s\mathbf{I} - \mathbf{A})^{-1}\} = \begin{bmatrix} 1 & t \\ 0 & 1 \end{bmatrix} \quad \ldots (10)$$

Now, the discrete fundamental matrix (discrete transition matrix) can easily be found simply by replacing the continuous time with a sampling time:

$$\Phi_k = \begin{bmatrix} 1 & T_s \\ 0 & 1 \end{bmatrix} \quad \ldots (11)$$

https://doi.org/10.1017/aer.2018.10 Published online by Cambridge University Press

The laser coordinator measures the LOS angle, and then a pseudo-measurement of relative position x_{1k}^* is created by multiplication of the LOS measurement by the range from missile to target:

$$x_{1k}^* = \lambda_k^* r \qquad \ldots (12)$$

And this is the measurement input to the Kalman filter. The discrete form of the measurement equation is:

$$\mathbf{z}_k = \mathbf{H}\mathbf{x}_k + \mathbf{v}_k = \begin{bmatrix} 1 & 0 \end{bmatrix} \begin{bmatrix} x_{1k} \\ x_{2k} \end{bmatrix} + \mathbf{v}_k = x_{1k} + \mathbf{v}_k, \qquad \ldots (13)$$

where $\mathbf{z}_k$ is the measurement vector (in our case, it is a scalar), $\mathbf{H}$ is the measurement matrix, and $\mathbf{v}_k$ is the noise measurement vector (which is also a scalar). Noise measurement is assumed to be zero mean Gaussian noise and the noise measurement matrix $\mathbf{R}$ is related to the noise measurement vector according to $\mathbf{R} = \mathrm{E}(\mathbf{v}\mathbf{v}^{\mathrm{T}})$, as mathematical expectation $\mathrm{E}(\cdot)$, and in this case, it is a scalar value $R_k = \sigma_n^2$, where σ_n^2 is the variance of the measurement noise.

The discrete form of control matrix is obtained from:

$$\mathbf{B}_k = \int_0^{T_\mathrm{s}} \Phi(t)\mathbf{B}(t)\mathrm{d}t = \begin{bmatrix} \dfrac{T_\mathrm{s}^2}{2} \\ T_\mathrm{s} \end{bmatrix} \qquad \ldots (14)$$

The applied Kalman filter calculates estimated values of the state vector. The Kalman filter outputs are given in the matrix form with the following recurrent formula:

$$\hat{\mathbf{x}}_k = \Phi_k \hat{\mathbf{x}}_{k-1} + \mathbf{B}_k n_{k-1} + \mathbf{K}_k (z_k - \mathbf{H}\Phi_k \hat{\mathbf{x}}_{k-1}) \qquad \ldots (15)$$

The previous expression can be written in another form:

$$\begin{bmatrix} \hat{x}_{1k} \\ \hat{x}_{2k} \end{bmatrix} = \begin{bmatrix} 1 & T_\mathrm{s} \\ 0 & 1 \end{bmatrix} \begin{bmatrix} \hat{x}_{1,k-1} \\ \hat{x}_{2,k-1} \end{bmatrix} + \begin{bmatrix} \dfrac{T_\mathrm{s}^2}{2} \\ T_\mathrm{s} \end{bmatrix} n_{k-1} + \begin{bmatrix} K_1 \\ K_2 \end{bmatrix} \left\{ z_k - \begin{bmatrix} 1 & 0 \end{bmatrix} \begin{bmatrix} 1 & T_\mathrm{s} \\ 0 & 1 \end{bmatrix} \begin{bmatrix} \hat{x}_{1,k-1} \\ \hat{x}_{2,k-1} \end{bmatrix} \right\} \qquad \ldots (16)$$

which can be further expanded as:

$$\begin{aligned} \hat{x}_{1k} &= \hat{x}_{1,k-1} + T_\mathrm{s}\hat{x}_{2,k-1} + \frac{T_\mathrm{s}^2}{2} n_{k-1} + K_1 \left[z_k - (\hat{x}_{1,k-1} + T_\mathrm{s}\hat{x}_{2,k-1}) \right] \\ \hat{x}_{2k} &= \hat{x}_{2,k-1} + T_\mathrm{s} n_{k-1} + K_2 \left[z_k - (\hat{x}_{1,k-1} + T_\mathrm{s}\hat{x}_{2,k-1}) \right] \end{aligned} \qquad \ldots (17)$$

These scalar equations of the Kalman filter can be presented graphically in the block diagram, as shown in Fig. 2.

The Kalman gains K_1, K_2 are computed in real time, while the filter is operating, from the matrix Riccati equations. The Riccati equations are a set of the following three recursive matrix equations.

https://doi.org/10.1017/aer.2018.10 Published online by Cambridge University Press

Covariance matrix $\mathbf{M}_k$, representing errors in the state estimates (i.e. the variance of real minus estimated values), after an update is:

$$\mathbf{M}_k = \mathbf{\Phi}_k \mathbf{P}_{k-1} \mathbf{\Phi}_k^{\mathrm{T}} + \mathbf{Q}_k = \begin{bmatrix} 1 & T_\mathrm{s} \\ 0 & 1 \end{bmatrix} \begin{bmatrix} P_{11} & P_{12} \\ P_{12} & P_{22} \end{bmatrix} \begin{bmatrix} 1 & 0 \\ T_\mathrm{s} & 1 \end{bmatrix} + \mathbf{Q}_k, \quad \ldots (18)$$

where the discrete process noise matrix $\mathbf{Q}_k$ can be found from the continuous process noise matrix and the fundamental matrix according to:

$$\mathbf{Q}_k = \int_0^{T_\mathrm{s}} \Phi(t) \mathbf{Q} \Phi^{\mathrm{T}}(t) \mathrm{d}t = \int_0^{T_\mathrm{s}} \begin{bmatrix} 1 & t \\ 0 & 1 \end{bmatrix} \begin{bmatrix} 0 & 0 \\ 0 & \Phi_\mathrm{s} \end{bmatrix} \begin{bmatrix} 1 & 0 \\ t & 1 \end{bmatrix} \mathrm{d}t = \Phi_\mathrm{s} \begin{bmatrix} \frac{T_\mathrm{s}^3}{3} & \frac{T_\mathrm{s}^2}{2} \\ \frac{T_\mathrm{s}^2}{2} & T_\mathrm{s} \end{bmatrix}, \quad \ldots (19)$$

where $\mathbf{\Phi}_\mathrm{s}$ represents the spectral density of the system noise, i.e. how much does one really trust to the mathematical model of the real system described by Equation (1).

The Kalman gains are:

$$\mathbf{K}_k = \mathbf{M}_k \mathbf{H}^{\mathrm{T}} (\mathbf{H} \mathbf{M}_k \mathbf{H}^{\mathrm{T}} + \mathbf{R}_k)^{-1} = \begin{bmatrix} M_{11} \\ M_{12} \end{bmatrix} (M_{11} + \sigma_n^2)^{-1} \quad \ldots (20)$$

The previous simplification comes from the fact that the covariance matrix in our case is a scalar $\mathbf{R}_k = \sigma_n^2 = (\sigma_\lambda r)^2$.

And finally, covariance matrix $\mathbf{P}_k$, representing errors in the state estimates before an update is given by:

$$\mathbf{P}_k = \begin{bmatrix} M_{11}(1 - K_1) & M_{12}(1 - K_1) \\ P_{12} & -M_{12}K_2 + M_{22} \end{bmatrix} \quad \ldots (21)$$

4.0 NUMERICAL SIMULATION

The simulation is performed for a non-manoeuvring target and in the vertical plane only. The 325 mm laser guided bomb has the mass, the axial moment of inertia and the transverse moment of inertia of 314 kg, 0.129 kg m^2 and 0.554 kg m^2, respectively. The total bomb length is approximately 2.55 m, the mass centre position referenced from the aft is approximately 1.44 m. Launching position of the aerial bomb is $x_0 = -3000$ m, $z_0 = -2000$ m, and angular orientation is determined only by the angle $\theta_0 = -33.69^\circ$ (directly toward the target–without the heading error, i.e.$HE = 0$). Angular rates are equal to zero, and initial bomb velocity $V_0 = 250$ ms^{-1} is only in bomb centreline direction. Perfect knowledge of relative missile to target range r and its rate V_c is assumed in simulations, so time-to-go and total time of flight can be computed as $t_\mathrm{go} = r/V_\mathrm{c}$ and $t_\mathrm{f} = r_0/V_{\mathrm{c},0}$, respectively. Sampling time is taken to be $T_\mathrm{s} = 0.05$ s, because the laser coordinator gives information on the target location 20 times per second.

In order to start the Kalman filter, we need initial covariance matrix P_0 for Ricatti equations calculation as the first filter tuning element. A particularly useful form of the homing loop

https://doi.org/10.1017/aer.2018.10 Published online by Cambridge University Press

model was given in Ref. 12, where only diagonal elements are used:

$$\mathbf{P}_0 = \begin{bmatrix} (\sigma_\lambda r)^2 & 0 \\ 0 & (V\ HE)^2 \end{bmatrix} \quad \ldots (22)$$

In the previous equation, the initial error in the estimate of position is simply the variance of measurement noise of our pseudo-measurement Equation (12), where the LOS angle, measured by the laser seeker, is corrupted with the assumed Gaussian noise of $\sigma_\lambda = 1$ mrad. The initial guess in the velocity error estimate is related to the missile velocity and the expected heading error (*HE*). The other filter tuning element is the process noise matrix $\mathbf{Q}_k$, where the process noise model is considered to be a target manoeuvre of constant amplitude with starting time uniformly distributed over the total time of flight. In Ref. 12, it was mathematically shown that the equivalent shaping filter is white noise through an integrator, so the spectral density of this white noise process is given by:

$$\Phi_s = \frac{w_0^2}{t_f} \quad \ldots (23)$$

In the case of a slowly manoeuvring target, we still have the gravity in the vertical plane, where the gravity compensation is included as an equivalent target manoeuvre, so take:

$$w_0 = g\cos\theta_0 \quad \ldots (24)$$

In Fig. 3, lateral displacements from the initial LOS are shown. In Fig. 4, lateral velocities, as the second state variable, for two different structures of the Kalman filter are presented.

After LOS rate estimation using Kalman filter, it is used as an input to optimal guidance law in order to get the commanded lateral acceleration as output from the optimal guidance law, as shown in Fig. 2. When the lateral acceleration is obtained, two cases may take place. In the first case, the filter had only information about the command (requested lateral acceleration) where the switch on the block diagram is in position 2. In the second case, an accelerometer is introduced in order to measure the achieved lateral accelerations; the switch is in position 1. It is observed that the second case gives better results, because in such way, the system lags are eliminated in actuators and in the airframe using the Kalman filter since it filters both commanded and achieved lateral acceleration. The final result is achieved after two consecutive filtrations of lateral acceleration.

In the following analysis, the effect of different guidance laws on trajectory shape and commanded lateral acceleration is given. Optimal guidance, proportional navigation, and guidance with the aerodynamic sensor are considered.

In the start point of the simulation, bomb–target distance is 6 km with LOS angle of $\theta_0 = -30^\circ$, i.e. $x_0 = -5196$ m, $z_0 = -3000$ m, and the bomb is launched with heading error of $HE = 4^\circ$ above the initial LOS.

Gravity compensation in the vertical plane has been introduced as an equivalent target manoeuvre influencing the term w_0 in Equation (7). According to Fig. 5, the obtained results from the trajectory simulation show a good agreement with those expected since they achieve the target. It is also remarkable that both PN and optimal guidance methods don't have a big curved trajectory unlike the pursuit guidance method which gives the most curved trajectory. From Fig. 6, it is clearly shown that the pursuit guidance method requires the largest amount of energy during the guidance phase, especially at the beginning. During the pursuit method

https://doi.org/10.1017/aer.2018.10 Published online by Cambridge University Press

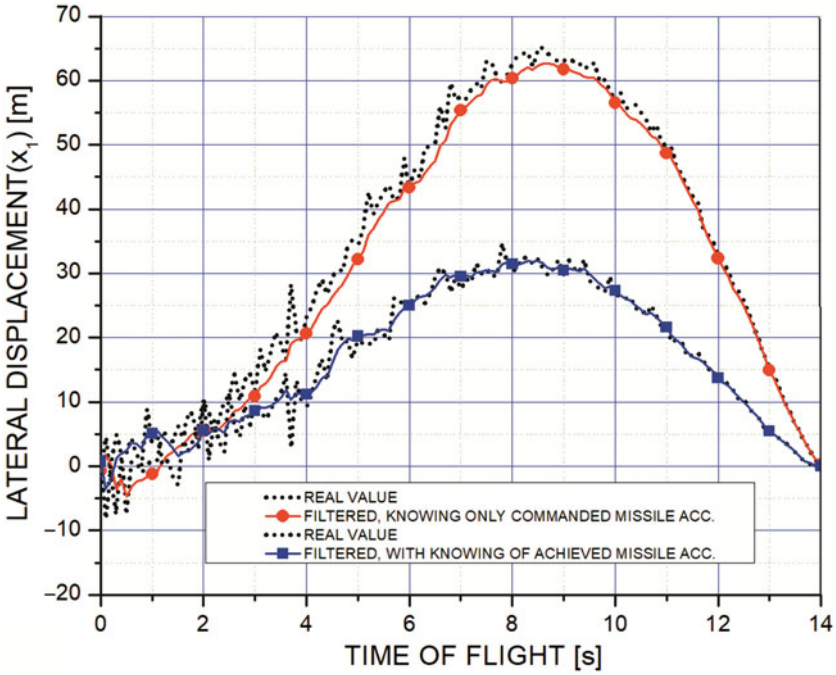


Figure 3. Lateral displacement (real and filtered).

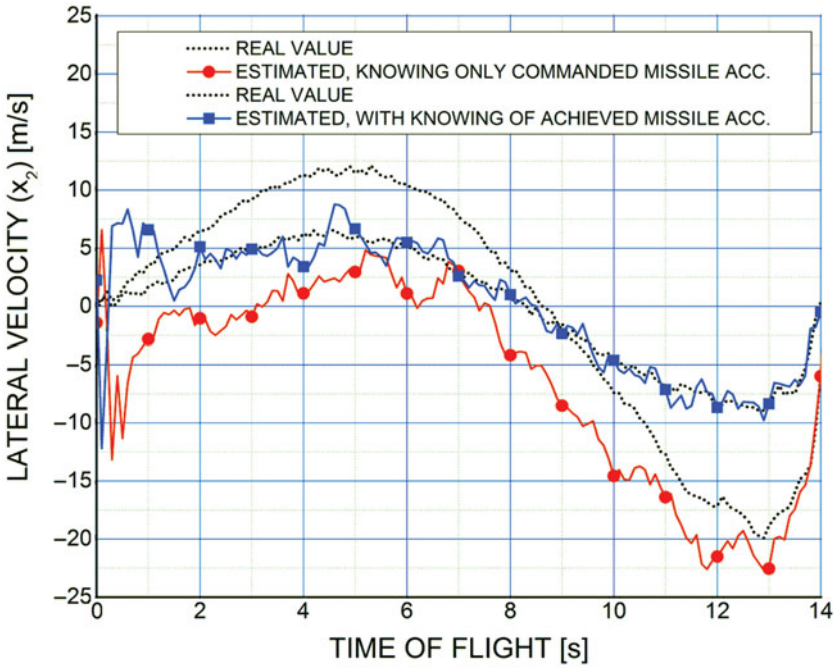


Figure 4. Lateral velocity (real and estimated).

https://doi.org/10.1017/aer.2018.10 Published online by Cambridge University Press

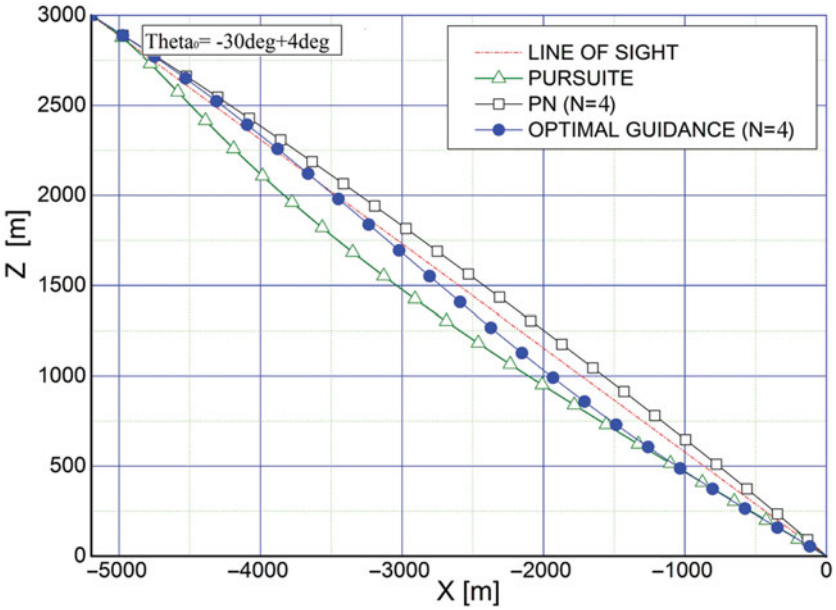


Figure 5. Trajectories for different guidance laws.

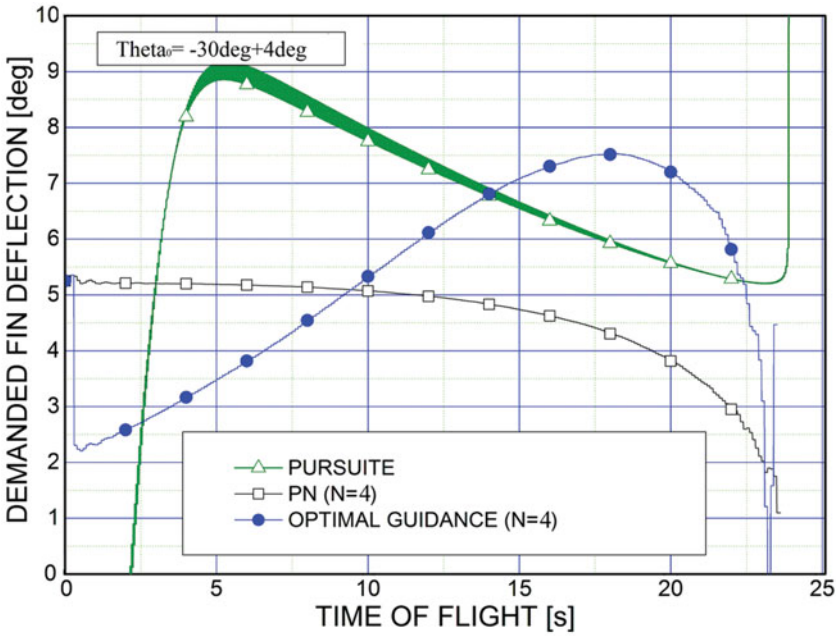


Figure 6. Strap-down (non-gimballed) homing head.

simulation, laser coordinator angle limitation has not been included because time flight limit is achieved while the target goes out of the field of view so that the guidance method cannot be used. Concerning the two remaining methods, PN guidance law and optimal guidance law, the common advantage is that they don't require a big amount of energy during the guidance

https://doi.org/10.1017/aer.2018.10 Published online by Cambridge University Press

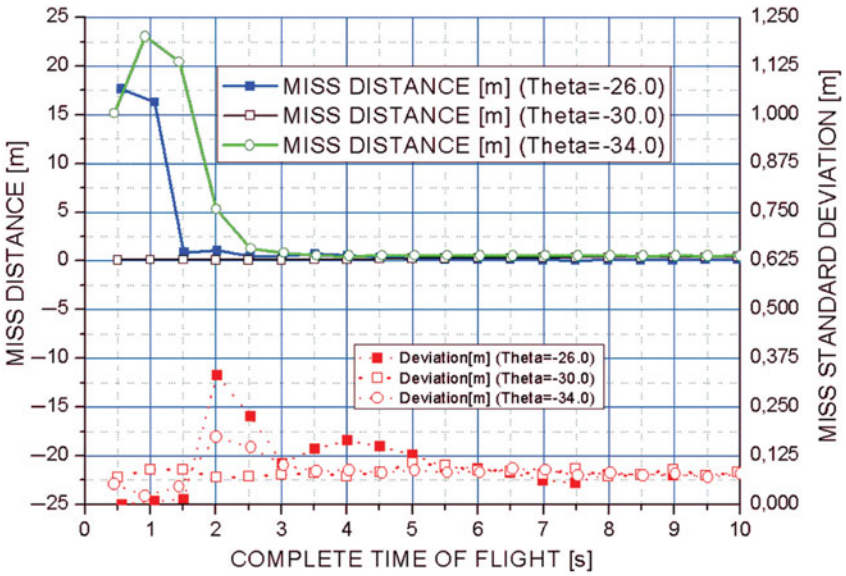


Figure 7. Terminal miss distance and deviation.

phase. However, the PN guidance law requires a complicated and expensive mechanical construction (gimballed homing head and tracking system) which justifies the use of the optimal guidance law to achieve the target with low cost and efficient system.

Statistical analysis of the optimal guidance method has been conducted by 50 runs of simulation execution for each total flight time in 0.5 s step increments, and miss distance has been considered in dependence on the total flight time. Analysed heading errors are -4°, 0°, 4°, and the results of an analysis are shown in Fig. 7.

Figure 7 shows that minimal time of flight has to be 4 s in order to achieve terminal miss distance less than 1 m. The corresponding minimal bomb-to-target launching distance is 1 km, for missile velocity of 250 ms^{-1}.

5.0 CONCLUSION

In this paper, the optimal guidance law for a laser guided aerial bomb is successfully applied. Filtering the measured values and estimation of the missing state variables are done by a second-order Kalman filter. It is shown that the measuring of the achieved lateral acceleration and its use in the structure of the filter is necessary to improve performance.

Comparative analysis of different guidance laws is done along with their performance in a realistic pursuer–evader engagement study and the advantages of some of them and faults of the others are shown. The complete research is very relevant in the context of the state estimation and missile guidance in a practical environment.

Statistical analysis is performed in order to get terminal miss distance as a function of total flight time. Limits of the minimal time of flight for the given miss distance are determined. In this way, the usability of the laser guided bomb with simplified mechanical construction and applied optimal guidance law are shown.

https://doi.org/10.1017/aer.2018.10 Published online by Cambridge University Press

In future work, time-to-go estimation should be considered without the perfect knowledge of relative range and its rate as assumed in this paper.

REFERENCES

1. DELONG, F., SUOCHANG, Y. and YINGXI, L. Research on missile system with strapdown guidance technology, *Advanced Materials Research*, 2013, **785-786**, pp 1560-1563.
2. YAO, J., WEI ZHOU, F. and WANG, X. Study of increment proportional guidance law for high maneuvering target, *Int J Signal Processing, Image Processing and Pattern Recognition*, 2015, **8**, (6), pp 181-192.
3. DAVID, K. and SOLOMON, R. Performance evaluation of proportional navigation guidance for low-maneuvering targets, *Int J Scientific & Engineering Research*, 2014, **5**, (9), pp 93-98.
4. PAVKOVIC, B., PAVIC, M. and CUK, D. Frequency-modulated pulse-jet control of an artillery rocket, *J Spacecraft and Rockets*, 2012, **49**, (2), pp 286-294.
5. KUN, C.-C., CHIANG, F.-L. and CHEN, K.-Y. Design a three-dimensional pursuit guidance law with feedback linearization method, *Int J Aerospace and Mech Engineering*, 2011, **5**, (7), pp 289-293.
6. DOWAN, K., CHANG-KYUNG, R., YONGHO, K. and JONGJU, K. Guidance and control for missiles with a strapdown seeker, Proceedings of the 11th International Conference on Control, Automation and Systems, October 2011, KINTEX, Gyeonggi-do, Korea.
7. JWO, D.-J., SHIH, J.-H., HSU, C.-S. and YU, K.-L. Development of a strapdown inertial navigation system simulation platform, *J Machine Science and Technology*, 2014, **22**, (3), pp 381-391.
8. SUN, T., CHU, H., ZHANG, B., JIA, H., GUO, L., ZHANG, Y. and ZHANG, M. Line-of-sight rate estimation based on UKF for strapdown seeker, *Hindawi Publishing Corporation Mathematical Problems in Engineering*, 2015, **2015**, (14) pp 1-14.
9. TAPAS, A., RAO, V. and PRABHAKAR, N. Adaptive estimation of line-of-sight rate measurement from a radio frequency seeker, *Defence Science J*, 2005, **55**, (3), pp 307-312.
10. BEN-ASHER, J.Z. Linear quadratic pursuit-evasion games with terminal velocity constraints, *J Guidance, Control, and Dynamics*, 1996, **19**, (2), pp 499-501.
11. GREWAL, M.S. and ANDREWS, A.P. *Kalman Filtering: Theory and Practice Using MATLAB, 4th ed., Wiley-IEEE Press, 2014*.
12. ZARCHAN, P. Tactical and strategic missile guidance, *Progress in Astronautics and Aeronautics*, 6th ed, American Institute of Aeronautics and Astronautics, 2012.

https://doi.org/10.1017/aer.2018.10 Published online by Cambridge University Press